

Committee 5
Non-linear Structures in Natural Science and Economics

Draft – January 1, 2000
For Conference Distribution Only



Non-linear Effects in the Model of Human Blood Coagulation

Alexei I. Lobanov
Associate Professor
Moscow Institute of Physics and Technology
Moscow, Russia

The Twenty-second International Conference on the Unity of the Sciences
Seoul, Korea February 9-13, 2000

Non-linear effects in the model of human blood coagulation

Alexei I. Lobanov

Moscow Institute for Physics and Technology
141700, Dolgoprudnyi, Moscow region, Russia.

E-mail: alexey@crimson.crec.mipt.ru

One of the most important achievements of XX century physics was the realizing of the key role of non-linear effects in nature. In particular, it is known that the genesis of non-linear objects – the solitons – depends on the interaction of non-linear effects and dispersion in the medium [1-3]. The work of Korteweg and De Vries became the foundation of the modern non-linear physics.

The same was the role of the work by Kolmogorov, Petrovskii and Piskunov [4], in which the wave in the medium where nonlinearity and dissipation compete with each other were discovered. The article, as well as [5,6], has been the impulse for the appearance of the number of works in which the generation of heterogeneous patterns caused by the loss of stability of the homogeneous state under the influence of diffusion, i.e. dissipative process, is studied.

The media, in which nonlinearity and dissipation lead to the pattern formation, as a rule described by the reaction – diffusion equations. For the different type of kinetics in the reaction terms these media are called as “active”, “excitable”, etc. It is characteristic for these media that the diffusion coefficients for activator and inhibitor are non-equal.

Recently the researchers paid their attention at the excitable media in which the process of recovery may have an autocatalytic character. Some results of the experimental investigation of the pattern formation dynamics during the human blood coagulation are given in [8]. It is necessary to pay the attention to the biochemical schemes of regulation, in which the inhibiting processes ruled by the activator, for the interpretation of the experimental data. Phenomenology of the blood coagulating paints both to the autocatalytic nature of the thrombin – the activator of the coagulating – and one of its inhibitor. There is none of considerable candidates at the role of such an inhibitor among the known coagulation metabolites.

The basic model. The system of partial differential equations describing the dynamics of human blood coagulation is considered as the basic model in the work [8]. The system is:

$$\frac{\partial \theta}{\partial t} = D \cdot \nabla^2 \theta + \frac{\alpha \cdot \theta^2}{\theta + \theta_0} - \kappa_1 \cdot \theta - \gamma \cdot \theta \cdot \varphi \quad (1)$$

$$\frac{\partial \varphi}{\partial t} = D \cdot \nabla^2 \varphi + \beta \cdot \theta \cdot \left(1 - \frac{\varphi}{C}\right) \cdot \left(1 + \left(\frac{\varphi}{\varphi_0}\right)^2\right) - \kappa_2 \cdot \varphi \quad (2)$$

The equations of the system describe evolution of concentration for two key metabolites: the activator of coagulation – thrombin – and the inhibitor (possibly protein C). Typical values of dimensional constants in the right side of the system (1)-(2) are given in the table.

Laplacian in 1D case is $\nabla^2 = \frac{1}{x^\nu} \cdot \frac{\partial}{\partial x} x^\nu \frac{\partial}{\partial x}$, $\nu=0$ corresponds to the plane case, $\nu=1$ – to the axially symmetric one. In the 2D case it is $\nabla^2 = \frac{\partial^2}{\partial x^2} + \frac{\partial^2}{\partial y^2}$. In the case of entire mixing ($D=0$) the equations of system (1)-(2) become the ordinary differential equations. This one is commonly called “pointed system”.

To the (1)-(2) we shall add also the equation of fibrin generation:

$$\frac{d\theta}{dt} = \theta \quad (3)$$

here is growth rate is assumed to be equal 1. The last equation reflects the fact that the activator of coagulating works as the catalyst for the polymerization. The fibrin concentration is the indicative value for us. The experimental data confirms that the presence of fibrin–polymer does not have influence on the molecular diffusion of metabolites.

Phase space (with the indication of zero-isocline) for the pointed system corresponding (1)-(2) is shown in Fig. 1.

Expression for zero-isocline can be explicitly written:

$$\varphi = \frac{1}{\gamma} \left(\frac{\alpha \theta}{\theta + \theta_0} - \kappa_1 \right) \text{ and } \theta = 0$$

$$\theta = \frac{\kappa_2 \varphi}{\beta \left(1 - \frac{\varphi}{C}\right) \left(1 + \frac{\varphi^2}{\varphi_0^2}\right)}$$

It can be easily seen that if $\alpha - \kappa_1 < C$ than there are three steady states. But only trivial one is stable. Any disturbance exceeding threshold value will grow with the time. This value may be approximately estimated as

$$\theta_{cr} = \frac{\kappa_1 \theta_0}{\alpha - \kappa_1} \quad (4)$$

Initially the autocatalytic growth of the activator concentration up to value θ^* exceeding the threshold one by for degrees. During the same time the inhibitor concentration scarcely achieves the inhibitor’s threshold φ_0 . Exceeding this concentration $\varphi(t)$ over φ_0

when $\theta(t) > \theta^*$ is accompanied by its blow up. Really, under the condition $C \gg \varphi \gg \varphi_0$, the growth rate of its generation may be approximately evaluated as: $\dot{\varphi} \cong \beta\theta^* \left(\frac{\varphi}{\varphi_0}\right)^2$, then for φ the following evaluation is considerable: $\varphi \sim \varphi_0 \cdot \left(\frac{1}{1-t/t^*}\right)$, where $t^* \approx \varphi_0/\beta\theta^*$ is the time of inhibitor's blow up.

Over-threshold disturbance of the activator is accompanied by the growth of its concentration by three or fore degrees. As a result, the second process – growth of the inhibitor's concentration – was started. The system of this kind we shall call *excitable media with active recovery*.

When the inhibitor concentration achieves its maximum value, the process of gradual recovery begins. First the concentration of activator decreases, after that – the inhibitor's concentration.

The character of mutual location of the isoclines changed when the model parameters modify. With growth of θ_0 disturbance threshold value θ_{cr} grows proportionally. When $\theta_0 = \theta_0^{bif}$ touching of zero-isoclines takes place, after that during the growth of θ_0 in the system is only one (trivial) steady state. The medium is stops to be excitable.

The evolution of the phase map during the changing of other parameters is also interesting. In particular, if θ_0 is fixed during the increase of φ_0 Andronov – Hopf bifurcation takes place. Unstable focus becomes stable and unstable limit cycle appears around it. The further changing of the value φ_0 is accompanied by the bifurcation of the appearance of the stable limit cycle from the separatrix loop. During the further increase of this parameter, the junction of two limiting cycles into one semi-stable cycle with multiplicity 2 takes place. Soon after that the last bifurcation takes place – the disappearing of the multiple cycle. In the system two stable states separating by the saddle is appear, the system became well-known trigger-type system.

In this range of parameters of the model we observed the well-known autowave phenomena – traveling waves, echowaves, similar to ones describing in [9]. We shall note that further we are deal with physiologically determined field of parameters, which are far from the values permitting the bifurcations described above.

Later in the focus of our attention there will be the questions connected with the mechanisms of the nonlinear waves generation and their behavior in the space-distributed

excitable media with active recovery. As a result of the preliminary investigation in 1D plane case, it was found that the mechanisms of the pattern formation in the proposed system has a number of distinctions from one in other active media, known earlier [8]. The pattern formation in the model is provided with the interaction of two autowaves – the activation wave and inhibition one. In this case, the second autowave is able to provide the stopping of coagulation and to interrupt the clotting even in homogeneous medium.

In the case $\theta \gg \theta_0$, equation (1) became the equation of heat conductivity with linear source. With the small inhibitor concentration the growth of activator propagation may be evaluated as:

$$V \sim \sqrt{(\alpha - \kappa_1)D_1}.$$

It is easy to be convinced that the equation (2) in the attitude to the variable φ , if the value of θ is fixed, is equivalent to the well-known Zel'dovich – Frank-Kamenetskii equation [10]. So the equation (2) is suitable for the description of inhibitor autowave propagation in the region where activator concentration is large enough.

Calculations in 1D case. In the numerical experiments the evolution of localized disturbances of the stationary state of the system $\theta \equiv 0, \varphi \equiv 0$ was considerate. In 1D calculations the initial perturbation was the step function according to activator:

$$\theta(x, t)|_{t=0} = \begin{cases} \theta_i, & 0 \leq |x| \leq l \\ 0, & l \leq |x| \leq L \end{cases}$$

where L – characteristics space size of the region, l – semi-width of the initial disturbance, θ_i is its amplitude. We search for solutions with zero-flux boundary conditions at $x = \pm L$.

The disturbances, which have small amplitude and/or small width, relax to trivial stationary state and are not able to initiate autocatalytic processes. The existence of the space size threshold is explained by the influence of the diffusion flux at the first stage of evolution.

They diminish activator amplitude until its value becomes smaller that threshold one. The problem of the initial disturbance parameter influence at the system evolution is observed more detail below.

In the case of considerably large initial disturbance both the diffusion and autocatalytic production of the activator take place in the system. Presence of both effects leads to propagation of the activator autowave set. The inhibitor stops the activator growth; but the production of the inhibitor has a time lag. This effect is due to 3 degree difference between constants of reactions growth rate α and β . As we can see from (2), the inhibitor autowave is able to propagate in the region where the activator concentration is high.

As a result of the reagents interaction initially localized activator concentration structure splits into two striations, which are symmetrical about the center of splitting ($x=0$), see fig. 2a. Concentrations of the metabolites gradually diminish, and the sharp fronts of autowaves smooth out by diffusion. The further evolution of the system depends on the model parameters. There are two different ways of the evolution.

In the first way the striations amplitudes become under - threshold, and the system comes into trivial steady state. As the sequence localized fibrin spot is formatted.

In the second way the activator quantity in the striations is enough for the initiation of self-accelerated processes of the activator production and its subsequent interaction with the inhibitor. Each striation divides into two new ones (see fig. 2b). In this case they may already be non-symmetric about new center of splitting because of the presence of the inhibitor generated at the previous stages of evolution. In contrast to the first splitting further three different types of the system behavior are possible.

- a) All the striations relax to the trivial stationary state. Fibrin structure consisting of three stripes in the plane case or a target of two rings in axially symmetric case is forming. It is should be noted, that the final number of fibrin elements may be more, that three. For example, when the equation's solution consists of the several periods type b) (see below) and finally the period of type a). It is important that the fibrin spots do not occupy the whole space, but only a finite part of it.
- b) The striations located nearer to the center of initial excitement of the system relax to the zero stationary state (see fig. 2c). The rest one again take part in the processes of growth and splitting with three alternatives shown here.
- c) The striations located nearer to the center of initial excitement of the system remain over-threshold. In this case the so-called kinetic echo effect takes place (see fig. 2d). As a rule, the growth and destruction of the inner striations take place in the same location where their predecessors were evolving. As a result, correspondent fibrin spot becomes more contrasts in comparison with the rest ones. Striations located further to the center of initial excitement may stay over- threshold and put their contribution into the further evolution as well as disappear.

When there is more than one blow up of the activator in the system evolution, then its evolution may be describe as the combination of several stage a), b) and c). In this case due to symmetry violation become of the presence of the inhibitor from the previous splitting acts the time of blowing up for different striation of the activator may be distinct. The amplitude of the striations differs as a consequence of it. Their evolution in the case of multiple

repeating of stage b) and c) will look like the autowave (traveling pulse or traveling wave generating the echowaves). In this case pulsations of the amplitude and propagating speed of the wave front set will be observed. All the regimes of the pattern formation may be classified in the following way:

The regime with the formation of one localized fibrin spot. This regime was briefly described above.

The regime of the traveling pulsing wave. This regime is multiple repeating of the b) scenario until the wave reaches the boundaries of considered space region. As a result periodical fibrin structure format. All spots have approximately same width and amplitude.

The regime of the echowave. In this case besides the activator wave propagating from the center of excitement the wave is form which travels to the reverse side. It, in its turn, may generate the second one propagating forward after the first autowave. More than that, one wave is able to generated a number of echowaves several times. The complex pattern is being formed which occupies the whole region considered. Some spots may have different amplitudes.

The regime with the generation of the fibrin pattern with the finite number of spots. This is the result of the combination of the stages b) or b) and c) ending with the scenario a), when the activator autowaves have not reach yet the borders of the space region. In the plane case we have a pattern consist of a several fibrin stripes, in the axially symmetric case – “target”. It is interesting the regimes of pattern formation similar to this one were observed in the experiments *in vitro* [8].

Dependence on the system parameters. The following parameters of the initial disturbance were chosen for calculations: $\theta_i=0.8$, $l=0.01(3)$ mm, $L=2$ mm. Values of all the system parameters except θ_0 , φ_0 were fixed.

In the fig. 3a the distribution of the different regimes on the parametric plane in 1D case is shown, in the fig. 3b it is shown for axially symmetric case. You can see that in the parametric (bifurcation) maps of the system the processes take place similarly concerning the quality. One can observe the propagation of the traveling waves with pulsing amplitude concerning time at the great values of the parameter φ_0 . There are regimes with the echowaves generating a little bit below. Further they are changed for the regimes with formation of a limiting number of fibrin spots. In our diagrams final structure with 4 or 5 patterns are related to the one region in the parametric map. These regimes are placed under

the echowaves. Possibly patterns with larger numbers of elements may be formatted, but they will be occupy more then 2 mm.

Below there are the regimes with formation of patterns with 3, 2 and 1 fibrin spots correspondingly. The echowaves from the extended tongue cutting the regimes with limit number of spots in the parametric map. The interchange of the regimes a little bit change higher and below of the tongue. The region of the formation three – elements pattern practically disappears above the tongue. The presence of the isolated points of other type regimes in the map indicates that it is present but becomes very narrow.

In the 1D plane case two tongues of the echowaves appear. One more tongue similar to the others appears above the first one. The boundaries of the transitional area between the echo and the limit number strips formation become twisting, isolated points on the map appear in the where the type of solution changed. The regime in which autoscaling is broken appear in the borders: The activator blowing up does not coincide along the co-ordinate with the place of former ones. The echowaves regime demonstrated the behavior characteristics for chemical turbulence [12]. The presence of such tongues probably indicates some resonance phenomena in the considered system.

Dependence on the initial conditions. Usually autowave systems or systems in which the pattern may be formatted, is possible show their properties without the way of medium excitement. It manifests itself in the fact that the solution of such a system does not depend on the initial conditions. It is only enough that the value of the initial disturbance shall exceed the value of its threshold [9]. Our calculations show more complex dependence upon the initial data for the model [13,14].

The dependence of the resulting regime of the value of integral parameter $I = \int_0^l \theta^2(x,t) dx$ at $t=0$ and on the semi-width of the initial step function l for 1D plane case are given in the following figures.

Regions in the fig. 4a,b corresponding to the different regimes are indicated the same way as the parametric maps. The threshold curve divides the plane $\{I, l\}$ into two areas. The disturbances above the threshold curve lead to the formation of different types of autowaves and patterns. From the threshold curve in fig. 4a the fan of curves dividing the over-threshold disturbance area into regions with different scenarios of pattern formation separates. Patterns with small quantity of elements, with one or two stripes correspond to the widest regions lying along the borders of the fan. There are the regions corresponding to the echo regime

and pattern formation scenarios from 3, 4 or 5 stripes inside the fan. We can see there narrow tongues like the parametric map. With the larger values of I , corresponding to the broader initial disturbances (fig. 4b) one more fan separates from the threshold curve. It has larger characteristics scale than the first one, but the tongues in it are less expressed.

Besides, the first fan separates from the threshold very sharply, its borders quickly appear on the vertical asymptotes. Curves in the second fan, on the contrary, have inclined asymptotes almost parallel to the threshold one.

Similar calculations were done also for 1D axially symmetric case. In fig. 5a one can see the splitting on the plane (I, R) , where $I = \int_0^R \theta(r, t = 0) r dr$, into the regions with qualitative different solutions in the case of small (I, R) . The “E” region corresponds to the echo regime, “1”, “2”, “3” and “4-5” correspond to the target pattern with respectively number of rings. In the fig. 5b the splitting of plane in the case of “large” initial disturbances can be seen. The indications are the same as fig. 5a.

Two-dimensional pattern formation. Taking into account that the system (1)-(3) depends on large number of parameters and the behavior of the solution essentially depends on the initial conditions, we did not have the goal to investigate and describe the whole variety of the 2D structures. Carried out calculations also show the presence of the repeating scenarios of its dynamic behavior. 2D fibrin patterns are forming during the interaction of two local heterogeneous striations. The evolution of such formations occurs in the same way. One traveling striation of the activator divided by the inhibitor into two similar ones, moving under some angle to the primary direction. The last ones staying over-threshold move away of the place of splitting. Later under the influence of inhibitor they, in their turn, split. We will briefly described results of two numerical experiments. More detailed description is given in [15].

“The interference” of disturbances from two sources. The dependence of the resulting clot form (in the experiments *in vitro*) on the distance between two sources of activator was one of the predictions of the hypotheses lying in the base of the model [16]. For the testing the series of calculations are carrying out. The parameters of the model were chosen as way as in 1D case the single polymer cloth was forming. Two isolated round clots were formed when the distance between the initial disturbances was large. When the distance was small, the final structure resembled the ones in experiments *in vitro* [8,17,18].

However, in some range of distances between two spots of initial disturbances the character of the pattern formation changed principally. After the growth of the activator concentration

and the generation of the inhibitor autowave two new sources at the same distance were formed, but they were turned of 90° in relation to their initial location. Further, some time later, because of the underthreshold heterogeneity of activator, caused by its several explosions the generation of moving lens-like striations. They are splitting and built the whole plane with the polymeric “ornament”.

In fig. 6 the activator concentration into the set moments of time are shown. The fibrin “ornament” in the final step of calculations is shown at the fig. 7.

The pattern formation with rotary symmetry. The presence of the repeating scenarios of dynamic behavior, self-similar elements, the growth rate and turn angle after splitting of which depends of kinetic parameters make us think about the possibility of existence of the final pattern with the rotary symmetry.

The dynamics of the activator concentration is shown at the fig. 8. The initial distribution is the ring with 5% concentration disturbance along the polar angle. One can see that the fibrin pattern performs layer by layer, every next one is being turned in relation with previous one. In the fig. 8 we can also see local centers of the symmetry of the fifth order – “the stars” of activator.

Summary. The simplest model of human blood coagulation described above demonstrated the variety of the dynamic behavior regimes. In this case solutions of the system depends on the initial conditions essentially. This fact isn’t shortcoming of the model. In contrast with many chemical and ecological models the different reaction to the different influences is physiological determined. The fact of autowave stopping in the homogeneous media directed by the chemical parameters is also interesting.

More detail information about the results obtained is in [11,13-15]. The problem of influence of advective flow on the coagulating processes is of a great interest both from the point of view of theoretical biophysics and medicine. The work of such modeling is being presently carried out.

Acknowledgments. The parts of the work are supported by Russian Foundation for Basic Research (the projects 99-01-01145, 99-04-48759)

The results represented in the work were obtained in co-operation with T. K. Starozhilova. The author was to express gratitude to T. K. Starozhilova and G. T. Guria for the participation in the work.

Table. The typical values of system parameters.

| | | | | | | | | | |
|---------------------------|--------------------------|---------------------------|-----------------------|------------------------|----------------|---------------------------|---------------------------|--------|--------|
| α, min^{-1} | β, min^{-1} | γ, min^{-1} | θ_0, nM | φ_0, nM | C, nM | χ_1, min^{-1} | χ_2, min^{-1} | $D_1,$ | $D_2,$ |
|---------------------------|--------------------------|---------------------------|-----------------------|------------------------|----------------|---------------------------|---------------------------|--------|--------|

| | | | | | | | | | |
|-----|--------|-----------------|-----|--------|-----|------|------|------------|------------|
| | | $\cdot nM^{-1}$ | | | | | | mm^2/min | mm^2/min |
| 2,0 | 0,0015 | 5,0 | 3,0 | 0,0525 | 5,0 | 0,05 | 0,35 | 0,0006 | 0,0006 |

Literature

1. R. K. Dodd, J. C. Eilbeck, J. D. Gibbon, H. C. Morris. Solitons and Nonlinear Wave Equations – Academic press Inc., London, 1982.
2. G. L. Lamb, jr. Elements of Soliton Theory – John Wiley & Sons, NY, 1980.
3. V. E. Zakharov et al, Soliton Theory. Moscow, Nauka, 1980 (in Russian).
4. A. N. Kolmogorov, I. G. Petrovskii, N. S. Piskunov //Bull. MGU, Mat. I Mekh., 1937, Vol. 1, Issue 6, pp.1-25 (in Russian).
5. A. M. Turing. // Phys. Trans. Roy. Soc. B., (London), 1952, Vol. 237, pp. 37-72.
6. G. Nicolis, I. Prigogine Self-Organization in Nonequilibrium systems. John Wiley & Sons, NY, 1977.
7. J. D. Murry Mathematical Biology. Springer, NY, 1989.
8. F. I. Ataulakhanov, G. T. Guria et al. //BBA, Vol. 1425 (1998), pp. 453-468.
9. V. A. Vasiliev, Yu. M. Romanovskii, D. S. Chernavskii, V. G. Yakhno. Autowave Processes in Kinetic Systems. Spatial and Temporal Self-Organization in Physics, Chemistry, Biology and Medicine. Berlin, VEB Deutscher Verlag der Wissenschaften, 1986.
10. Ya. B. Zel'dovich, D. A. Frank-Kamenetskii //Dokl. Akad. Nauk SSSR, 1938, Vol. 19, p. 693 (in Russian).
11. G. T. Guria, A. I. Lobanov, T. K. Starozhilova //Biophysics, 1998, Vol. 43, N 3, pp. 526-534.
12. T. Yamada, O. Kuramoto //Progr. Theor. Physics, 1976, Vol. 56, N 2 pp. 681-683.
13. A. I. Lobanov, T. K. Starozhilova //Matematicheskoe Modelirovanie, 1997, Vol. 9, N 12, pp. 3-15 (in Russian).
14. A. I. Lobanov, T. K. Starozhilova //Phystech Journal, 1997, Vol. 3, N 2, pp. 96-104.
15. T. K. Starozhilova, A. I. Lobanov, G. T. Guria //Matematicheskoe Modelirovanie, 1997, Vol. 9, N 2, pp. 21-25 (in Russian).
16. F.I. Ataulakhanov, G.T. Guria //Biophysics, 1994, Vol. 39, N 1, p.92-96.
17. F.I. Ataulakhanov, G.T. Guria, A. Yu. Safroshkina //Biophysics, 1994, Vol. 39, N 1, pp. 97-104.
18. F.I. Ataulakhanov, R. I. Volkova, G. T. Guria, V. I. Sarbash //Biophysics, 1995, Vol. 40, N 6, pp. 1320-1328.

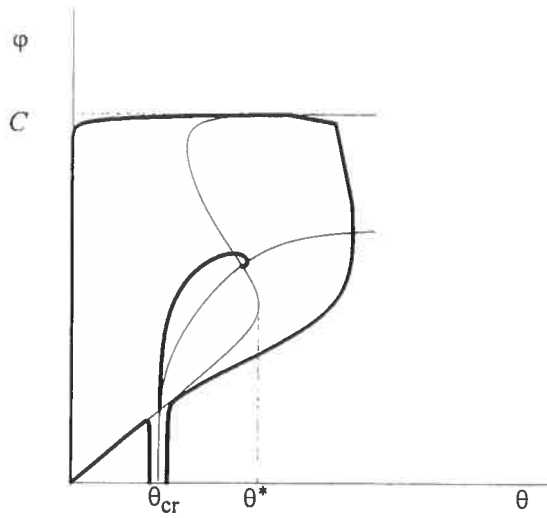


Fig. 1. The phase plane of the point system. The zero isoclines are shown by thin lines. The thick lines show phase trajectories. The scales of the axes are non-linear. $\theta_0 = 5,0$ nM; $\phi_0 = 0,05$ nM; other parameters see in the table.

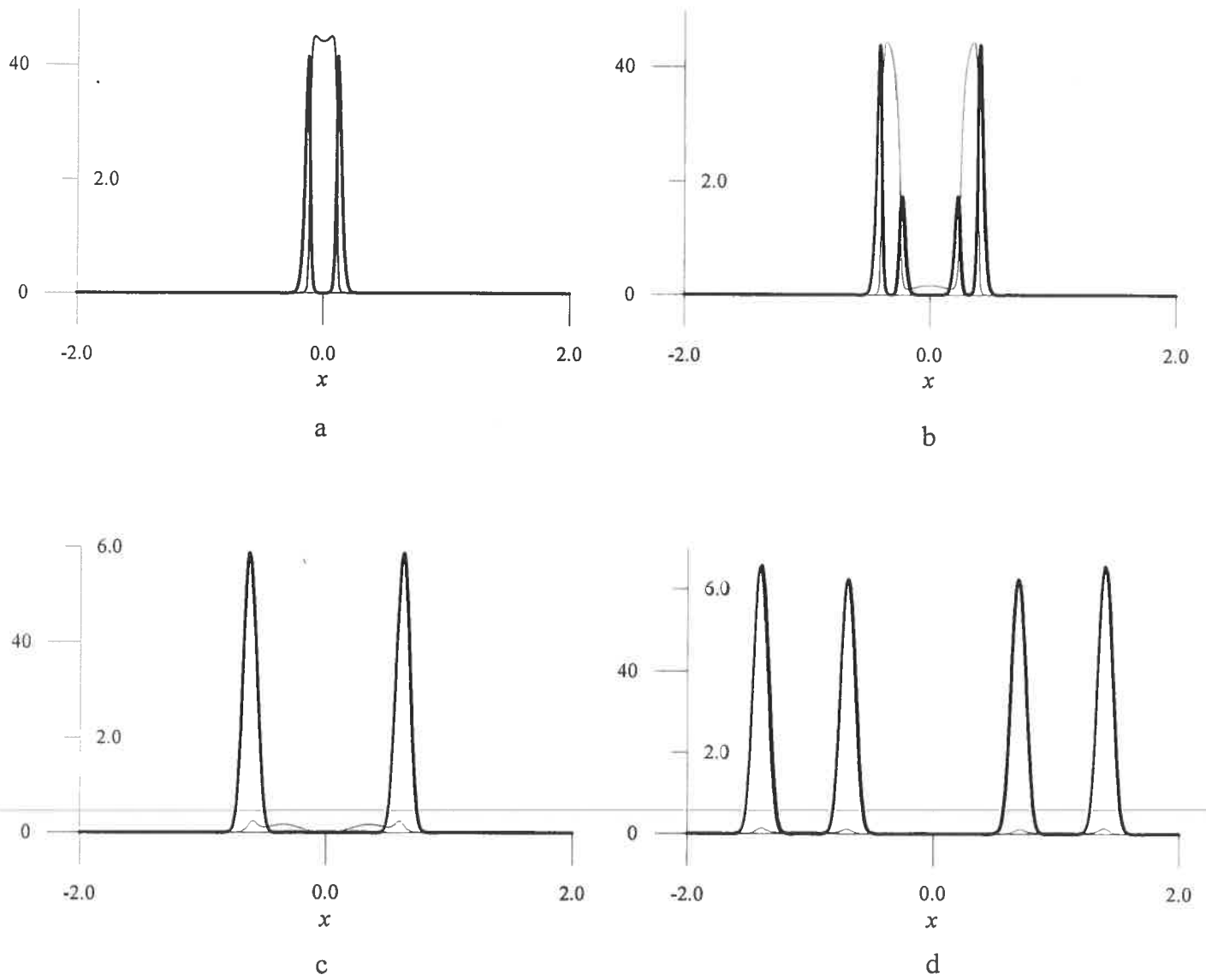


Fig. 2. The evolution of striations *a*: $t = 5'4''$, *b*: $t = 16'9''$, *c*: $t = 25'0''$, *d*: $t = 101'36''$. The thick lines show activator distributions, the thin lines — inhibitor. $\theta_0 = 3,0$ nM. For *a*, *b*, *c* $\varphi_0 = 0,065$ nM and for *d* $\varphi_0 = 0,056$ nM. Other parameters see in the table.

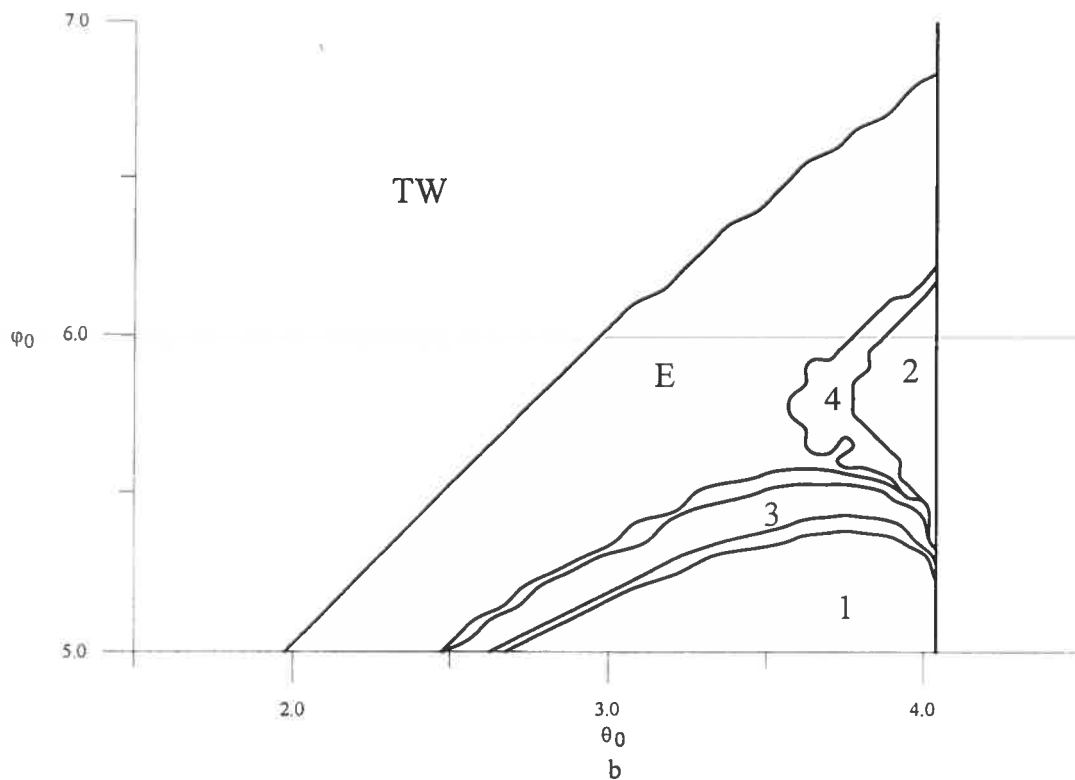
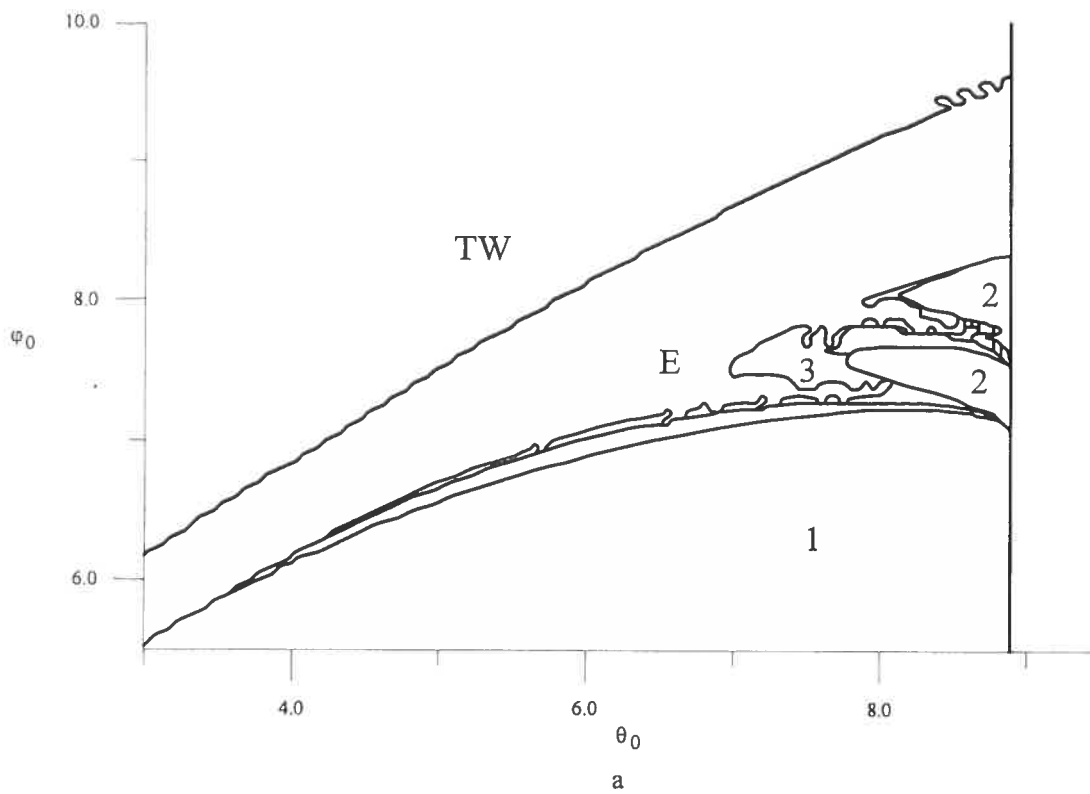


Fig. 3. Parametric maps of the system *a*: in 1D plane case; *b*: in 1D axially symmetric case. E-region corresponds to echowave, 1, 2, 3 — to pattern formation with the corresponding stripes or rings number. $[\theta_0] = 1 \text{ nM}$, $[\varphi_0] = 10^{-2} \text{ nM}$.

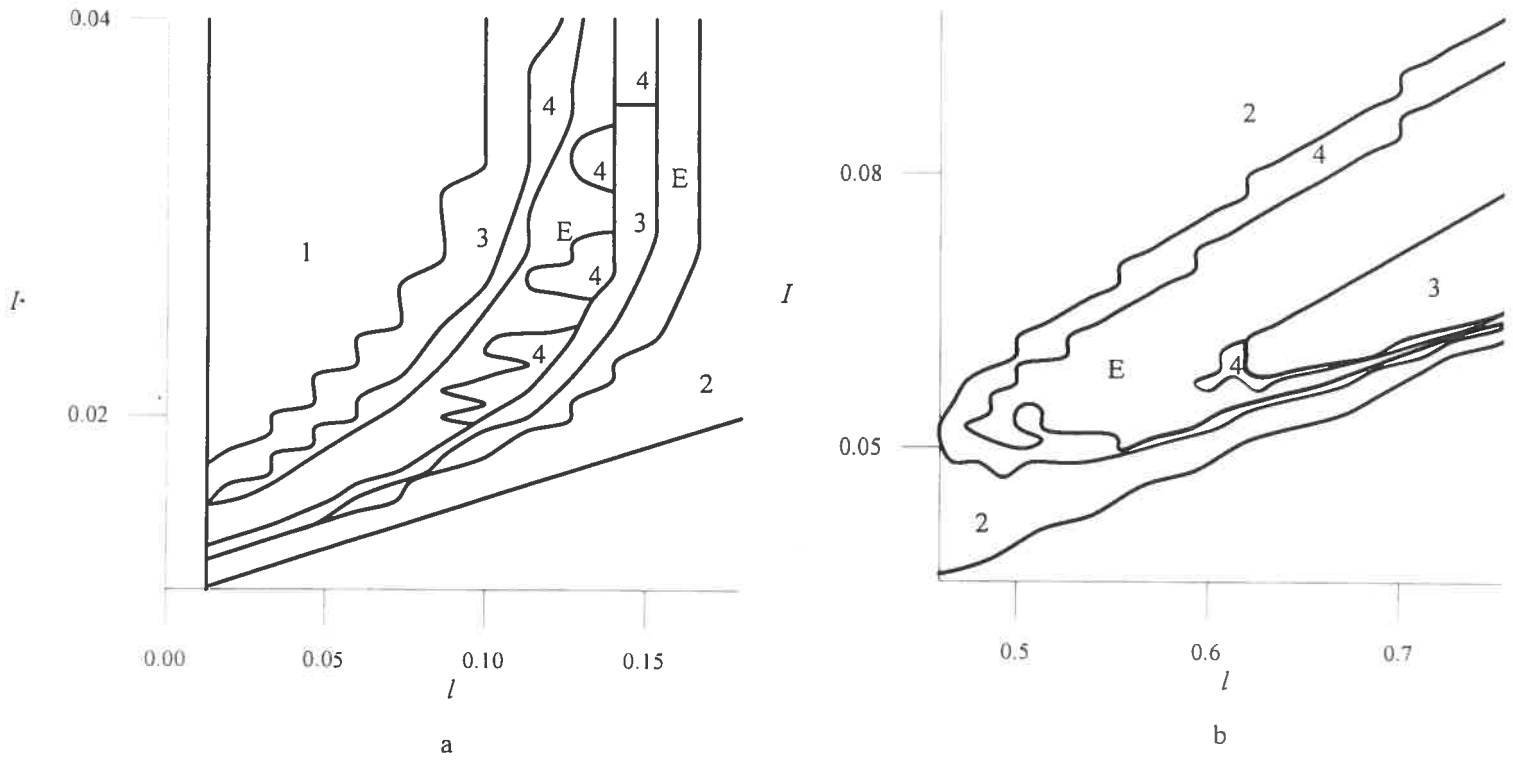


Fig. 4. The dependence on the initial conditions in 1D plane case. Designations of the regimes are the same like at Fig. 3. Parameters see in the table.

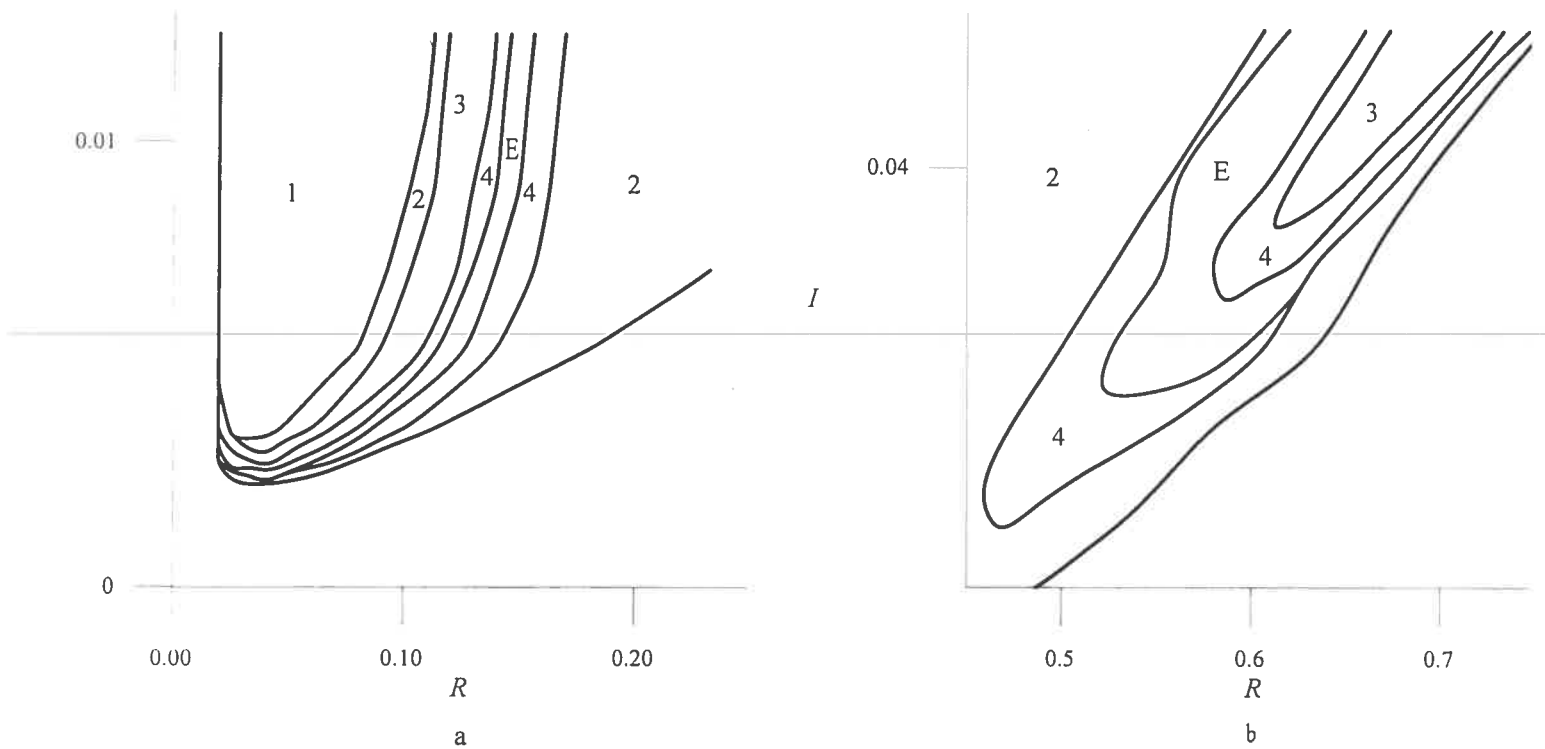


Fig. 5. The dependence on the initial conditions in 1D axially symmetric case. Designations of the regimes are the same like at Fig. 3. Parameters see in the table.

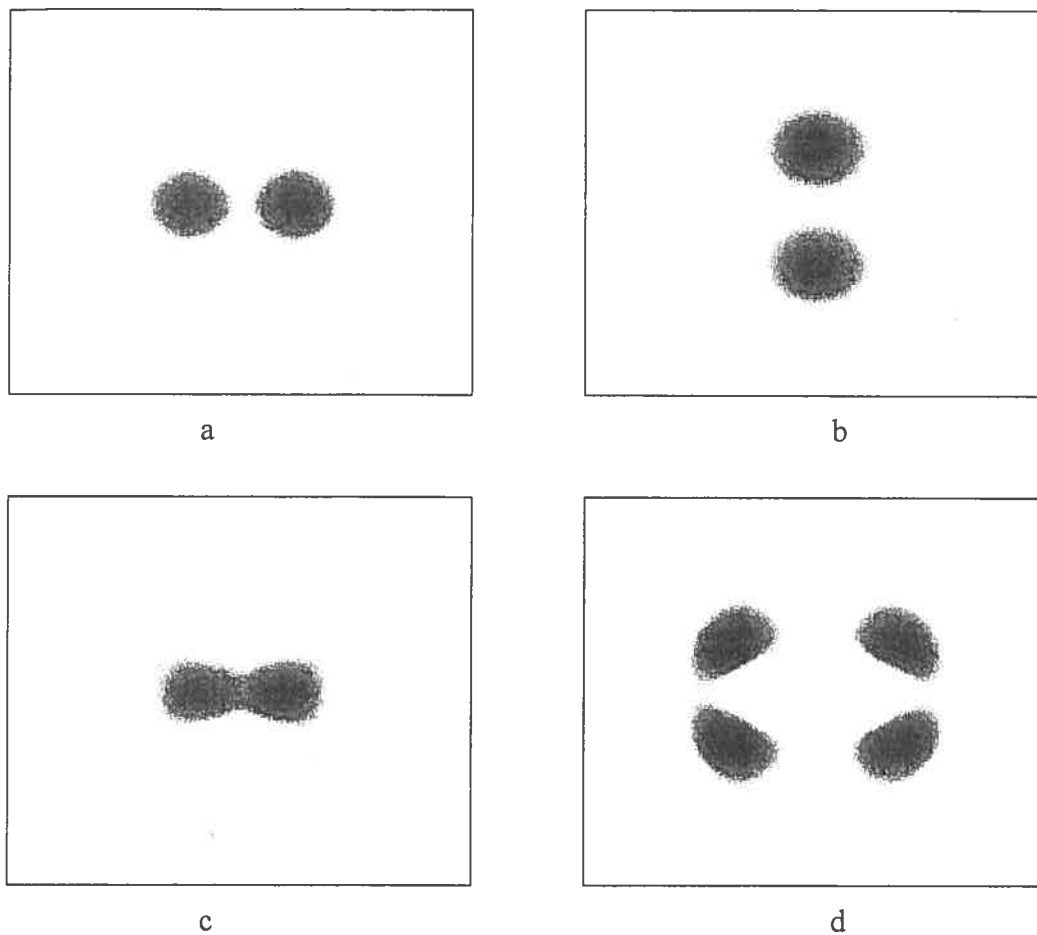


Fig. 6. The distributions of the activator in the process of 2D pattern formation *a*: $t = 20'$, *b*: $t = 58'$, *c*: $t = 72'$, *d*: $t = 82'$. $\theta_0 = 3,95 \text{ nM}$, $\varphi_0 = 0,05325 \text{ nM}$. The domain size was $2 \text{ mm} \times 2 \text{ mm}$ with a grid of 200×200 points, time step $t = 0,01'$. The initial perturbation was two circle steps with amplitude of $0,8 \text{ nM}$, width $0,067 \text{ mm}$ placed on $0,47 \text{ mm}$ from each other.

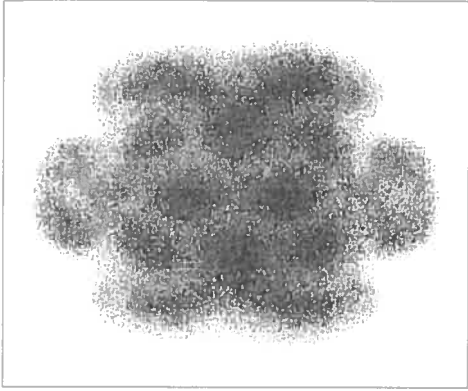


Fig. 7. The distributions of the fibrin in the process of 2D pattern formation shown in the Fig. 6. $t = 82'$.

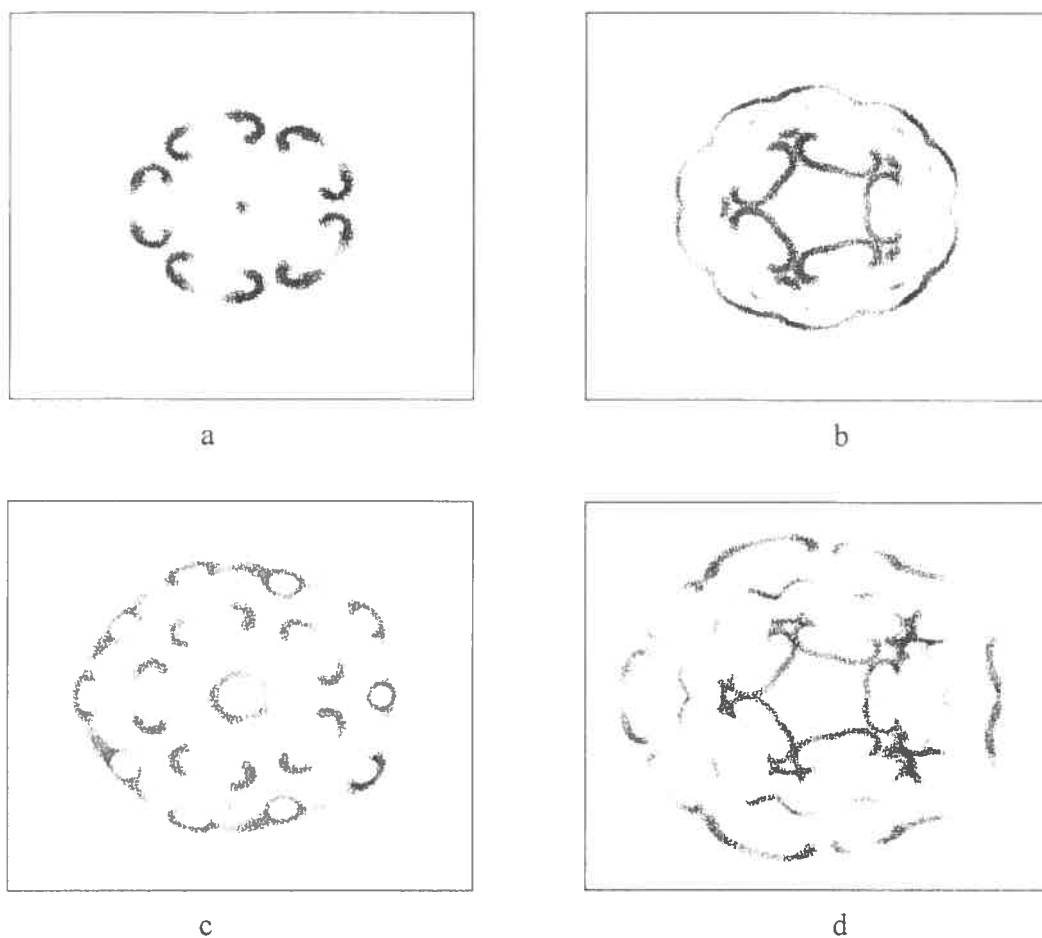


Fig. 8. The distributions of the activator in the process of 2D pattern formation *a*: $t = 19'$, *b*: $t = 29'$, *c*: $t = 36'$, *d*: $t = 47'$. $\theta_0 = 3,10 \text{ nM}$, $\varphi_0 = 0,0565 \text{ nM}$. The domain size was $2 \text{ mm} \times 2 \text{ mm}$ with a grid of 200×200 points, time step $t = 0,01'$. The initial perturbation was a ring with amplitude of $0,8 \text{ nM}$ and 5% variation along the polar angle. The radii of the ring were $0,5 \text{ mm}$ and $0,4 \text{ mm}$.